Proceedings of the Twenty-seventh (2017) International Ocean and Polar Engineering Conference **www.isope.org**
San Francisco, CA, USA, June 25-30, 2017

ISBN 978-1-880653-97-5; ISSN 1098-6189

Design and Dynamic Performances of Y-Wind Floating Offshore Wind Turbine Platform

Sung Youn Boo, Steffen Allan Shelly, Daejun Kim
VL Offshore LLC
Houston, USA

ABSTRACT

A semi-submersible type floating wind turbine platform with 5MW power rate called "Y-Wind" is newly developed to improve the dynamic performances by employing damping plates. The platform is moored at a water depth of 200m with three catenary chain lines. Time domain coupled simulations are conducted to assess the dynamic responses for the various design load cases including power production, extreme and survival conditions. The present Y-Wind design is also validated with the ABS design requirements. Significant reductions of motions are observed due to the damping plates, which also results in reducing the mooring line tensions, compared to the values with no damping plate hull.

KEY WORDS: Y-Wind; damping plate; dynamic response; mooring; offshore floating wind turbine; semi-submersible

INTRODUCTION

The majority of the current offshore wind turbine farms are located in the shallow water with fixed foundations although there are many opportunities to take advantages of deepwater wind farms with floating foundations. The offshore floating foundations to harvest the wind energy could be designed by applying the mature technologies of the oil and gas platforms in the hull, mooring, installation, and many associated areas. Various types of floating foundations have been developed and can be categorized into semi-submersible, spar, TLP, and barge. The designs have been evolved mainly to minimize the wave-wind coupled interactions by typically implementing large displacement hull, heave plate, deep draft hull or high tensioned vertical mooring system. Example designs are OC4 Semi (Robertson et al., 2014), Windfloat (Rodierr et al., 2010), Trifloater (Antonutti et al., 2014), CSC-Semi (Xu, 2015), VolturnUS (Viselli, 2015b), Hywind (Statoil website; Jonkman, 2010), and Pelastar (Hurley and Nordstrom, 2015). Like the oil and gas platforms, the cost drivers of the floating wind foundations are the fabrication, mooring and installation costs so that the platform design should consider the acceptable hull size to be fabricated in the existing yards, integrated at quayside, and towed and installed with no expensive vessel in order to lower the cost. In addition, disconnection from the mooring and tow to yard can be considered for a critical damage repair to the turbine: Large sized or deep draft hull may suffer from the fabrication yard limitations or installation vessel requirement whereas foundations with insufficient self-buoyancy like TLP may need dedicated vessel from tow to installation. As for those factors, the floating foundation designs suggest a comprehensive design approach with provisions in a series of phases from the concept design to installation and maintenance.

A semi type Y-Wind platform (foundation) has been designed typically for US offshore application considering all the aspects stated above. With iterations, optimum platform size to fit in the US ship yards but still to produce the maximum power is derived, which is identified to be 5 to 6MW platform. For the present study, Y-Wind with 5MW is selected. The Y-Wind platform has three offset (outer) columns connected to a center column with the respective pontoon. The center column supports the turbine tower. The columns and pontoons are sized accordingly to give a proper lightship draft considering the US shipyard water depth, but maintaining a sufficient stability from the tower integration at quayside to the platform installation at site. The Y-Wind design is further improved with adding damping plates to the platform keels. The damping plates can increase the viscous damping mostly in the heave motions and help to shift the motion resonance zone away from the dominant wave energy zone. The damping plate schemes have been applied to the floating wind platform and can be found in Rodierr et al. (2010), Antonutti et al. (2014), Cheema et al. (2014), Lopez-Pavona et al. (2015) and Cermelli et al. (2010) for the semi, and Kim et al. (2014) for spar platforms.

The Y-Wind is a braceless platform benefitted from an efficient production of the hull, less loading due to environment and no deck air-gap issues, although there are susceptible zones in stress near the pontoon connections which can be resolved accordingly. A few platforms have adopted the breaceless design concept, for instance, VolturnUS semi (Viselli, 2015b), CSC Semi (Xu, 2015) and V-Shape semi (Fukushima FORWARD, 2014; Karimirada and Michailides, 2015).

The present study considers three different Y-Wind hull configurations: no damping, narrow and wide damping plates where the hull principal dimensions of those configurations remain unchanged. The platform dynamic performance analyses are conducted for the design conditions

of the power production, 50-yr extreme and 500-yr survival conditions. The associated metocean conditions used for the present analysis are derived from typical US offshore data available. Natural periods of motions, RAOs and damping ratios for the design conditions are compared for the three configurations and damping plate effects are addressed. Further simulations are carried out to access the dynamic responses in horizontal and vertical accelerations, roll and pitch angles and mooring line tensions. The Y-Wind designs are validated with the design criteria of the floating wind turbine recommended by ABS (2015).

METOCEAN CONDITIONS

Offshore platform designs utilize site specific metocean data and the same approach can be applied to the floating wind platform design. However, the wind platform site is not available so that for the present study the environmental data combining the data of US offshores including Gulf of Mexico, East and West coasts are derived, based on the references (ABS, 2013; Weinstein, 2014; Viselli et al., 2015a; Viselli et al., 2015b), and summarized in Table 1. JONSWAP spectrum is chosen and its associated peak enhancement factor of Gamma with each Design Load Case (DLC) is given. Water depth considered is 200 m. Fig. 1 presents the current profiles along the depth derived with the surface speed and proper ratio along the water depth implementing the GoM West profiles for water depth>150 m (API, 2007).

The DLCs in Table 1 are in accordance with ABS (2015). The operating (power production) condition is in the speed ranges from V_r (cut-in) to V_o (cutout) wind speed while the turbine will be parked or idle under the 50-yr extreme and 500-yr survival conditions.

Table 1. Metocean Data

Platform Condition	Operating		Extreme	Survival
ABS DLCs	1.3	1.6	6.1	SLC
Environ. Condition	V_r	V_o	50-yr	500-yr
Turbine Condition	Prod.	Prod.	Parked	Parked
Wind @ 10m (m/s)	9.2	19.0	29.1	32.3
@ hub (m/s)	11.4	25.0	40.0	45.0
Wave Hs (m)	7.5	8.5	12.5	15.0
Tp (s)	11.5	13.7	14.2	15.3
Gamma	1.0	2.2	3.3	3.3
Current @ Surface (m/s)	0.4	0.6	0.8	1.0

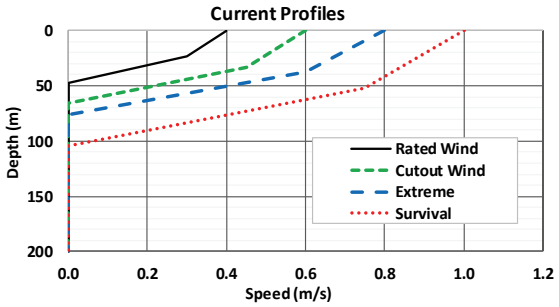

Fig. 1 Current Profiles for operating, extreme and survival conditions

DESIGN REQUREMENTS

The Y-Wind platform is installed in the US offshore at a water depth of 200 m and designed to produce a power of 5MW for a service life of 25 years under the sea environments specified in Table 1. The platform with the tower integrated at a quayside in US shipyards has a sufficient self-buoyancy to support the platform at a low wet-tow draft, which enables the tow-out of the platform from the yard to site with no dedicated vessels.

The mooring system and air-gap of Y-Wind platform will comply with the ABS requirements (ABS, 2015; ABS FPI 2013; ABS Guidance Note, 2014; API, 2005) which are presented in Table 2. The extreme (DLC 6.1) and survival (SLC) design criteria are used for mooring line safety and air-gap assessments (ABS, 2015). The selected mooring safety factor of 2.0 for extreme is for non-redundant intact while 1.05 for survival is for non-redundant or redundant intact mooring lines. In addition, the platform rotations and accelerations in operating conditions (DLCs 1.3 and 1.6) are considered such that the rotor-nacelle assembly components are prevented from a potential damage during the power production. For the present design, the allowable platform rotation and nacelle acceleration are selected 10 deg and 0.4g (3.92 m/s^2) respectively, considering the engineering practices in oil and gas offshore platform designs. Other design values of rotation and acceleration for the floating wind turbines can be found in Huijs et al. (2014) and Suzuki et al. (2011).

Table 2. Y-Wind Floating Turbine Platform Design Criteria

DLCs	Heel (deg)	Accel. (g)	Mooring FoS	Air Gap (m)
Operating (1.3, 1.6)	≤ 10	≤ 0.4	-	-
Extreme (6.1)	-	-	≥ 2.0	≥ 1.5
Survival (SLC)	-	-	≥ 1.05	≥ 0.0

Y-WIND PLATFORM CONFIGURATION

The Y-Wind semi type platform is designed to produce the sufficient buoyancy with a smaller lightship draft such that the tower and rotor assembly can be integrated to the platform at quayside in US fabrication yard and towed to the site with conventional tugs. Also at the design stage, a static heel angle of the platform due to the mean rotor thrust at the rated wind speed is considered such that the static heel angle is maintained below 4 deg. In addition, it is checked if the platform has a sufficient positive metacentric height specifically in wet-tow and ballasting operations. Various damping structure options are considered in order to improve the platform dynamic responses. All these design parameters are implemented to the in-house platform sizing program to configure the four-column semi type Y-Wind platform and the resulting platform particulars are compared in Table 3, where No DP, Narrow DP and Wide DP means platform with no damping, narrow and wide damping plates respectively. The damping plates are attached to the keel of the platform. Additional descriptions of the conceptual sizing can found in Boo et al. (2017). Fig. 2 represents the Y-Wind platform moored with three catenary mooring lines, where the damping plates are omitted.

The total weight of the platform was estimated considering the hull structure, appurtenances, marine growth, ballast, turbines and marine system, where an appropriate contingency was applied based on the past experiences of the oil and gas platform design. Lightship draft with the tower and rotor assembled is about 5.2 ~5.3 m. No active ballast is required during the power production.

Table 3. Y-Wind 5MW Platform Particulars

Items	Units	No DP	Narrow DP	Wide DP
Displacement	tonnes	7,748	7,761	7,770
Draft – Design	m	18.0	18.0	18.0
Offset Column Center Radius	m	35.0	35.0	35.0
Column OD	m	10.5	10.5	10.5
Outer Column Height	m	29.5	29.5	29.5
Center Column Height	m	28.0	28.0	28.0
Freeboard (Out. Column)	m	11.5	11.5	11.5
Pontoon Width / Height	m	4.5 / 4.0	4.5 / 4.0	4.5 /4.0
Pontoon Height	m	4.0	4.0	4.0
Tower Base above SWL	m	10	10	10
Hub Height above SWL	m	90.0	90.0	90.0
CoG (above keel)	m	14.58	14.41	14.23

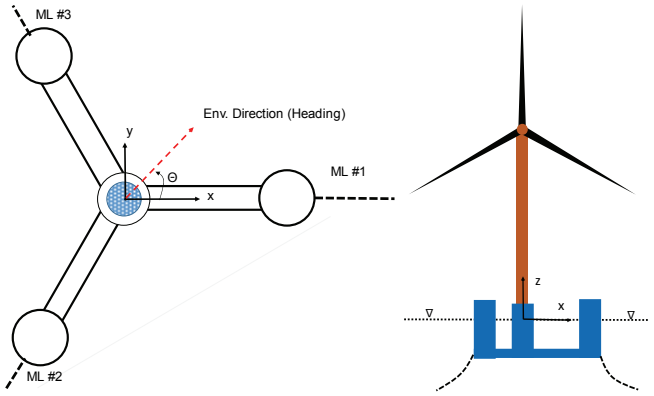

Fig. 2 Y-Wind Platform Coordinate System Definition

The NREL 5MW reference wind turbine (Jonkman et al., 2009; Robertson et al., 2014) was selected and its properties are summarized in Table 4. The tower base and hub are located at 10m and 90m above still water line (SWL) respectively. The rotor thrusts at the rated and cut-off wind speed presented in Table 4 were used to assess a static heel angle due to the mean thrust at the platform design stage.

Table 4. NREL 5MW Wind Turbine Data

Power Rate	MW	5
Rotor Diameter	m	126
Number of Blades	-	3
Tower Height	m	77.6
Tower Diameter Top / Base	m	3.87 / 6.5
Cut-in V_{in} / Rated V_r / Cut-out V_{out}	m/s	3.0 / 11.4 /25.0
RNA Weight	tonnes	350
Tower Weight	tonnes	250
Rotor Thrust - Rated Wind	KN	819
- Cutout Wind	KN	369

NUMERICAL MODELING

Y-Wind platform coordinate systems and environment direction used for the present analysis are presented in Fig. 2. The reference center is located at the platform center on the SWL. Wave direction (heading) is positive toward the x-direction and measured in counter-clock wise direction. Mooring Lines (ML) #1 to #3 with a 120 degree apart are also shown in Fig. 2.

The Y-Wind platform columns and pontoons below the SLW were modelled with source panels for the radiation and diffraction analysis. The damping plates were discretized with the dipole panels assuming its thickness is very thin. The platform is moored with a total of three catenary R4 studless chain lines with 120 mm diameter at a water depth of 200 m. There will be no redundant mooring line with the present mooring configuration so that the mooring safety factor shall be chosen accordingly as presented in Table 2. Minimum Breaking Load (MBL) of the uncorroded chain is 13,573 kN. The one end of the 800m long line is connected to a fairlead located near the keel of the outer column and the other end is connected to an anchor foundation. MBL of corroded chain due to corrosion over the service life of 25 years was utilized to assess a factor of safeties of the mooring strength.

Wind forces on the hull above the SWL and wind turbine tower were estimated based on the reference (ABS FPI, 2013) and input to the numerical model in terms of wind coefficients. The current loads on the submerged platform members and the mooring lines were represented in the model with the drag coefficients given in Table 5. Hull viscous damping was also presented in the model with the viscous drags implementing the drag coefficients of columns, pontoons, damping plates and mooring lines. The column Cd are chosen 0.65 (Ishihara and Waris, 2012). Vertical Cd of 1.5 of the column was based on the experimental data (Fisher, 1998). Drag coefficients on the pontoon also vary with the aspect ratio (breadth / depth) and Kuelegan-Carpenter number. The horizontal and vertical Cds on the pontoons were read from the experimental data plot in reference (Venugopal, et al, 2009). According to DNV (2007), a recommended Cd of a square cylinder is about 2.2 for Reynold number$\approx 4.7\times10^4$. Damping plate drag coefficients on the vertical direction was selected to be 4.5, which is little lower than the values used in references (Robertson at al., 2014; Li et al, 2012).

Table 5. Platform Members and Mooring Line Drag Coefficients

Column - Horizontal / Vertical	0.65 / 1.5
Pontoon – Horizontal / Vertical	1.9 / 2.2
Damping Plate - Vertical	4.5
Chain - Normal / Tangential	2.4 / 1.15

The present time-domain numerical analyses were carried out using Orcaflex. In this study, a semi-coupled analysis with neglecting the aero-elastic couplings was implemented (ABS Guidance Note, 2014). The tower and nacelle were modeled as part of the rigid body of the hull. The rotor thrust loads were modeled by applying the respective static loads in Table 4, at the top of the tower for the power production cases of DLC 1.3 and 1.6 in Table 1. This approach is very useful in practical sense to evaluate the platform global performances and mooring responses in the early design stages although it does not provide the dynamic responses of tower and accurate aero-hydro coupled effects to the platform.

NUMERICAL RESULTS AND DISCUSSIONs

Heave Free Decay Tests

Fig. 3 compares the heave and pitch free decay test time histories of the platforms with no DP, narrow DP and wide DP. It can be seen that the damping plate effects are more significant in the heave than the pitch motions. Roll decays are omitted in the comparison due to similarity to the pitch motions. The Y-Wind platform natural periods (T_n) of

motions are summarized in Table 6, where natural period increase ratios (%) of narrow DP and wide DP to the no DP periods are also compared. Significant period changes (24% increase with narrow DP and 41.5% with wide DP from no DP) are found in heaves, which is resulted in increase of the platform added mass induced by the damping plate. Considerable increases of the roll and pitch natural periods with wide DP can also be observed. Mooring line damping contributions to the heave motions are compared in Fig. 4. According to these comparisons, no noticeable mooring damping effects in heave motions are observed except the no DP case where very small mooring damping contributions are presented.

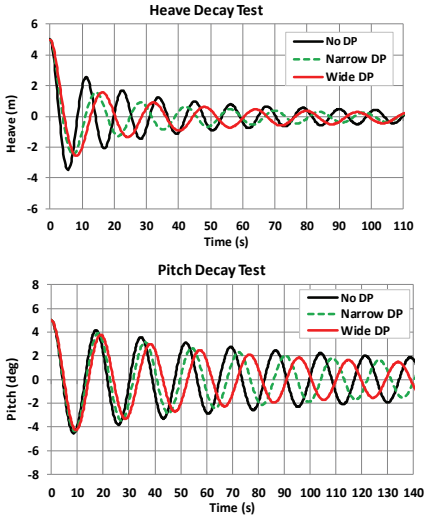

Fig. 3 Time Histories of Heave and Pitch Free Decays

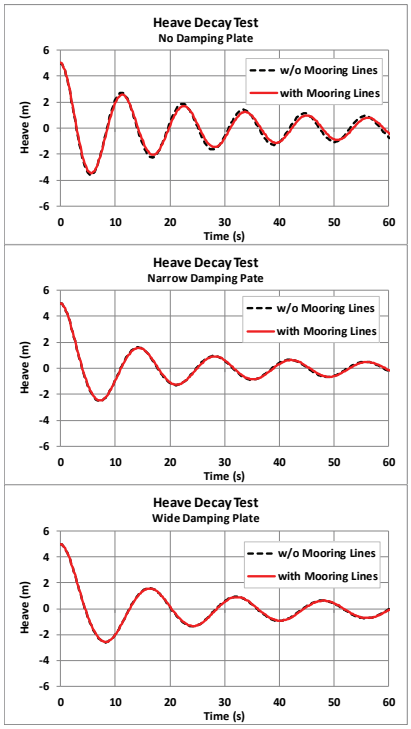

Fig. 4 Comparison of Heave Decays with and without Mooring Lines (top: No DP, middle: narrow DP, bottom: wide DP)

Table 6. Natural Periods of Y-Wind Platform

Motion	No DP	Narrow DP		Wide DP	
	T_n (s)	T_n (s)	% increase	T_n (s)	% increase
Surge	177.18	181.03	2.2	182.68	3.1
Sway	177.28	181.13	2.2	182.78	3.1
Heave	11.25	13.95	24.0	15.92	41.5
Roll	17.38	18.12	4.3	19.18	10.4
Pitch	17.35	18.12	4.4	19.15	10.4
Yaw	101.07	102.25	1.2	103.27	2.2

Damping Ratios

Logarithmic decrement δ and damping ratio ζ can be computed every cycle using equations;

$$\delta = ln\,(A_{c\,i} / A_{c\,i+1}) \text{ or } \delta = ln\,(A_{t\,i} / A_{t\,i+1}) \quad (1)$$

$$\zeta = \delta / 2\pi \quad (2)$$

where $A_{c\,i}$ and $A_{c\,i+1}$ ($A_{t\,i}$ and $A_{t\,i+1}$) are two consecutive crest (or trough) values in the decay time histories (Fig. 5). However, this method gives different decrement values for each cycle depending on the selection of the crest or trough peaks if the peaks are offset from zero. To minimize a possible offset effect, a peak-to-peak method can be utilized to compute the logarithmic decrements (Butterworth et al, 2004) as;

$$\delta = ln\,[(A_{c\,i} - A_{t\,i}) / (A_{c\,i+1} - A_{t\,i+1})] \quad (3)$$

An example comparison of heave logarithmic decrements for two different methods for the no DP case in Fig. 3 is made in Fig. 6. The decrements from the crest and trough from Eq. 3 differ much in the first few cycles, whereas the peak-to-peak method (Eq. 3) could provide the values in sense of averaged decrement.

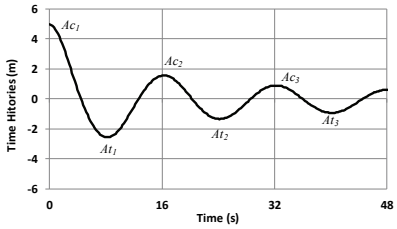

Fig. 5 Example Time Histories

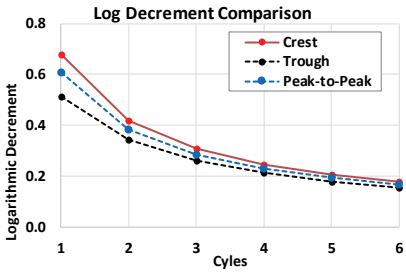

Fig. 6 Comparison of Log-Decrements of Heave Motions (no DP)

Total damping ratios of the Y-Wind platform to the critical damping, utilizing the peak-to-peak method are illustrated in Fig. 7, up to first 6 cycles of the decay time histories. Initial displacements of the decay tests are 10 m for surge and sway, 6 m for heave and 5 deg for roll, pitch and yaw respectively. The time histories of the heave and pitch used are presented in Fig. 3.

As observed in the free decay tests, the damping plate attributes to the heave most, and then roll and pitch in magnitude. The damping plates give very small influences to the surge, sway and yaw as similar results are reported in Ishihara and Waris (2012). It is interesting that the heave damping effects of the narrow and wide DPs are very similar to each other while the roll and pitch motions are dampened more with the wide DP than with the narrow DP. This heave, roll and pitch combined actions induced by the wide DP could contribute to improve the platform responses in the severe sea states, compared to the narrow DP case. It could be stated that the heave motions are dampened with the hull viscous damping mostly induced by hull structural members and damping plates. More prominent damping in heave and roll (pitch) occurs at the initial few cycles, indicating that higher amplitude of motions can create the bigger dampening motions. The associated drag coefficients used for the analyses (Table 5) will be correlated using the model test data when available.

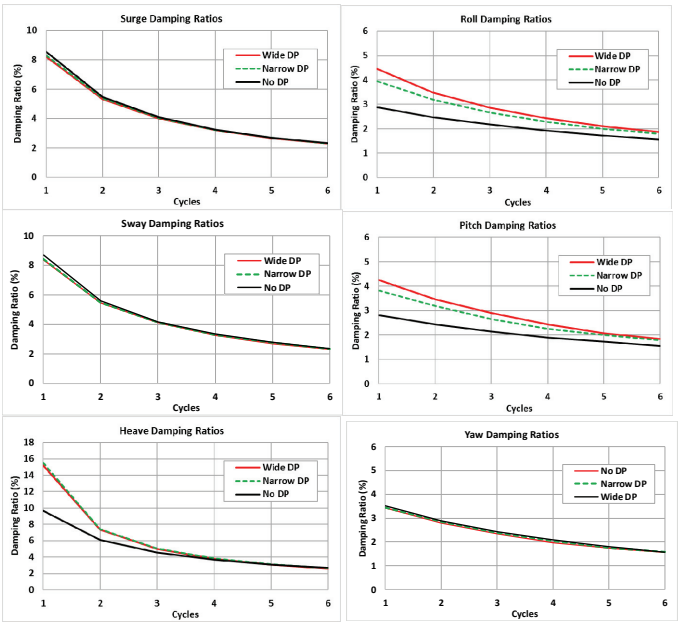

Fig. 7 Damping Ratios vs. Cycles of Y-Wind Platforms

Platform and Mooring Tension RAOs

White Noise (WN) waves with Hs 2.0 m and heading 180 deg were used in the numerical model for RAO estimations. No wind and currents were considered. Fig. 8 compares the heave and pitch RAOs of Y-Wind platforms with no DP, narrow DP and wide DP. Also RAOs from potential-based diffraction analysis with potential damping are presented together in Fig. 8. Shifts of the peaks toward higher periods occur due to the increased added mass by the damping plates. Significant reductions of the heave and pitch responses near the resonances by the viscous dampings are observed. Fig. 9 compares the horizontal and vertical acceleration RAOs at the nacelle. Those acceleration peaks coincide with the platform pitch and heave resonance periods, respectively. The acceleration peak reduction ratios with the damping plates are more pronounced in the vertical than the horizontal direction which is accounted for higher damped motions in heave than pitch. Additional tests with Hs 6.0 m were also carried out and the damping effects of the motions and accelerations were found to be greater than the present cases with Hs 2.0 m. However, those results are not reported in this paper. As also seen in Fig. 8 and Fig. 9, the platform with the wide damping plate is superior to other platforms configured with no DP and narrow DP.

Given the wave heading of 180 deg, the most loaded line is mooring line #1 (ML#1). Its tension RAOs are, thus, compared in Fig. 10. The tension RAO peaks are located at two locations of around the platform heave and pitch resonances, indicating that the mooring tensions are influenced by both motions of heave and pitch (or roll for 90 deg heading), together with the low frequency motions which are not captured in the plots. This implies that the combined effects of heave, pitch (or roll) and rotor actions can also cause the mooring line fatigue damages but these are not covered in this study.

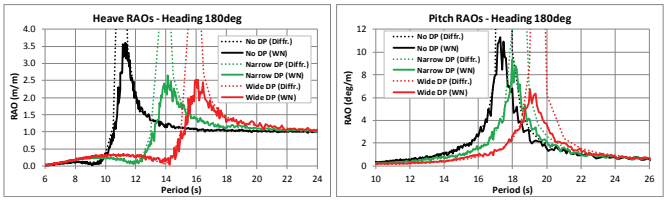

Fig. 8 Heave and Pitch RAOs

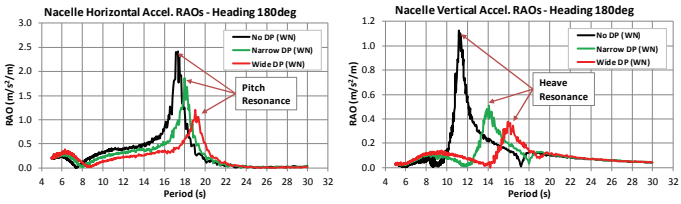

Fig. 9 Nacelle Horizontal and Vertical Acceleration RAOs

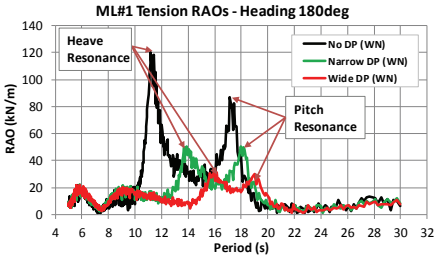

Fig. 10 ML #1 Tension RAOs

Dynamic Response Assessments

Numerical simulations were performed to evaluate the dynamic responses with four environmental headings of 0, 90, 135 and 180 deg. Wind and currents were codirectional to the waves. The metocean conditions in Table 1 were used for the present analysis. Time domain simulations were run for three hours excluding initial ramp-time and post-processed to compute the statistics of the simulations. Extreme values can be determined with Rayleigh 3-hour most probable extreme by,

$$Most\ probable\ Max = \mu + \sigma\,[2\ ln(n)]^{½} \quad (4)$$

or 3-hour extreme with 1% risk factor by

$$Max = \mu + \sigma\,[2\ ln(-n/ln(1-\alpha))]^{½} \quad (5)$$

where $n = T/T_z$ is the number of peaks and T, T_z, μ, σ and α are the storm duration, mean up-crossing period, mean, standard deviation and risk factor, respectively. All the results presented in this section are based on the most probable maximum except the mooring line tensions which used 1% risk factor extreme.

Heave and pitch power spectral densities for the design load cases of operating (rated), extreme and survival are compared in Fig. 11. It is seen that heave and pitch motions in the operating condition are governed by the platform resonance periods whereas the motions in the extreme and survival conditions by the wave periods

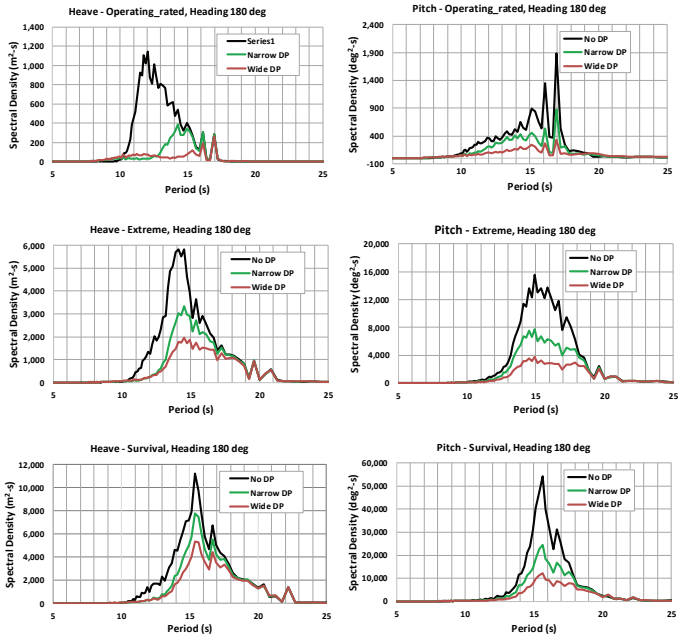

Fig. 11 Heave and Pitch Response Spectra (Heading 180 deg)

Fig. 12 compares the single amplitude heave motions of the Y-Wind platforms for the operating (rated and cutout), extreme and survival conditions with no DP, narrow DP and wide DP, showing that the heave motions increase as the sea states increase. Mark symbols within each DLC represent all the extreme values obtained from the heading 180, 135, 90 and 0 deg in order as depicted in Fig. 13 and these notations are applied to the following plots. Fig. 12 also shows that the damping plate contributes to the heave reductions for all the considered DLCs. The large heave motions combined with the pitch roll (roll) may affect the air-gap at the deck of the platform under the extreme and survival condition but the airgap evaluation was skipped as Y-Wind platform has no deck structures.

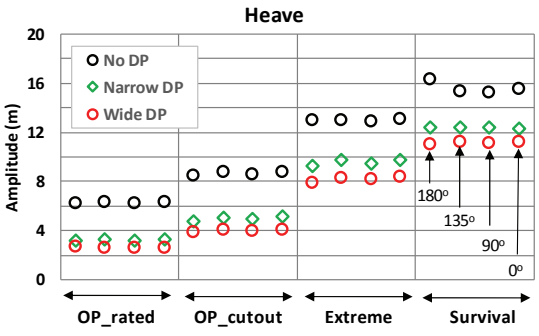

Fig. 12 Heave Amplitudes under the Various DLCs

Pitch motions of mean and extreme for four headings are presented in Fig. 13 and Fig. 14. Maximum mean pitch is about 3.3 deg at the rated wind and 1.4 deg at cut-out wind speeds. The maximum mean pitches from the dynamic simulations are lower than the static heel angle of 4 deg considered in the platform sizing stage, which is likely due to the combined actions of the mooring, current and wind induced moments. The pitch extreme values increase in the higher sea states but the maximum for the operating (rated and cutout) conditions is found to be lower than the allowable pitch of 10 deg, which demonstrates that the platform pitch design requirement is complied with. The maximum roll and pitch motions of the platform without the damping plate under the extreme and survival seas are very large compared to the values with the damping plate, which proves that the damping plate especially wide DP works well in the pitch (roll) along with the heave.

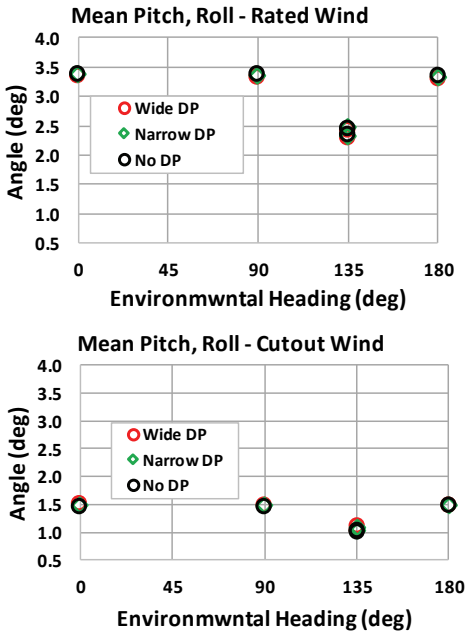

Fig. 13 Comparison of Mean Pitch Amplitudes under the Various DLCs

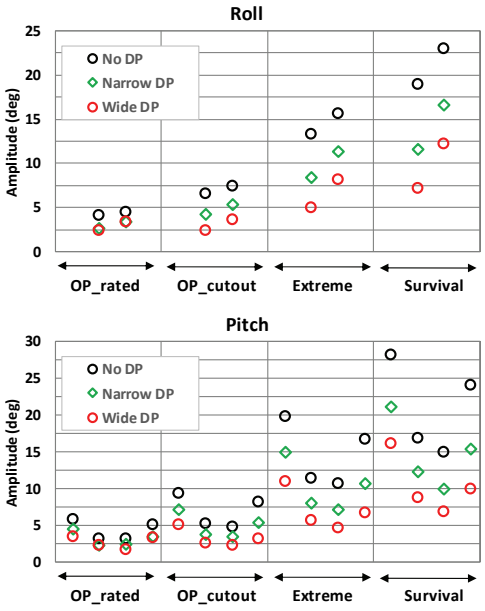

Fig. 14 Comparison of Extreme Roll and Pitch under the Various DLCs

Vertical and horizontal accelerations at the nacelle under the various DLCs are compared in Fig. 15. The accelerations of the platform with the damping plate during the power production is well below the allowable design maximum of 0.4g. Higher horizontal than vertical accelerations are observed, which is mainly induced by the pitch (roll) motions under the extreme and survival conditions.

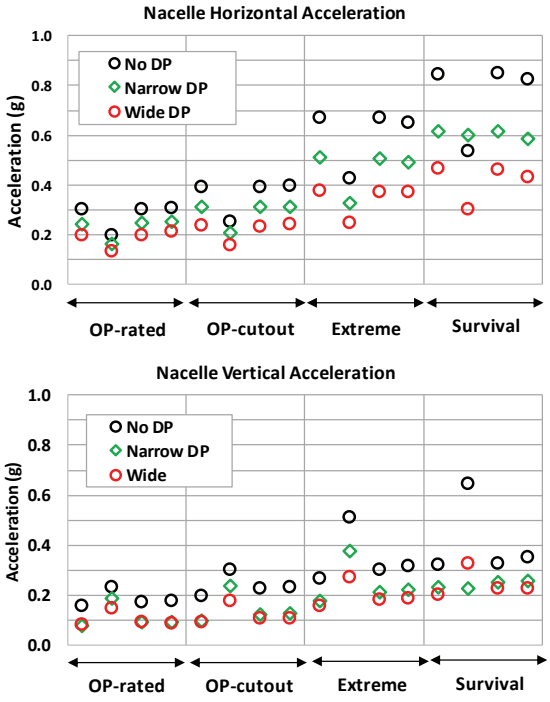

Fig. 15 Nacelle Extreme Accelerations under the Various DLCs

Mooring line Factor of Safety (FoS) at the fairlead was estimated for all three lines under the considered four headings and the results are illustrated in Figs 16 to 19. As described earlier, the mooring FoS was based on the MBL of the corroded chain. The mooring FoSs under the extreme and survival seas become much smaller than the operating seas, due to higher dynamic motions. The mooring strengths of the platform with the damping plates comply with the ABS mooring design requirements in both extreme and survival conditions given in Table 2. It also indicates that the platform with the wide damping plate produces less dynamic tensions than other platforms, which could be resulted in the reduced dynamic motions in heave, roll and pitch by the damping plate. This reduced tension results are very promising in the platform structural and anchor designs.

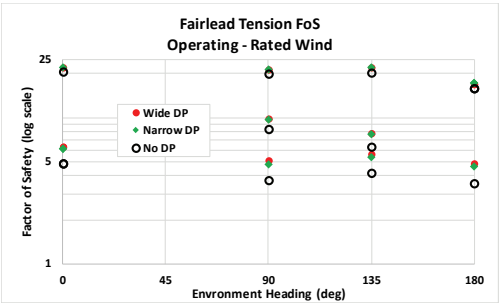

Fig. 16 Mooring Line Factor of Safeties: Operating (Rated Wind)

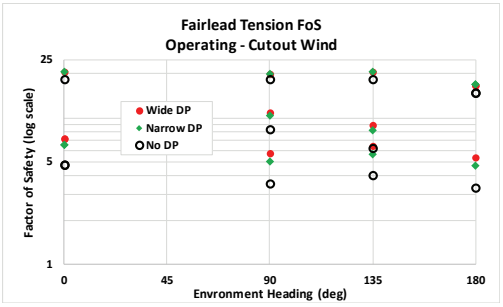

Fig. 17 Mooring Line Factor of Safeties: Operating (Cutout Wind)

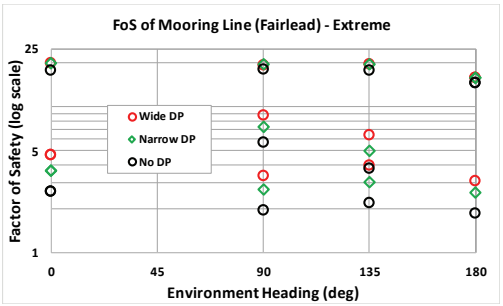

Fig. 18 Mooring Line Factor of Safeties: 50-yr Extreme

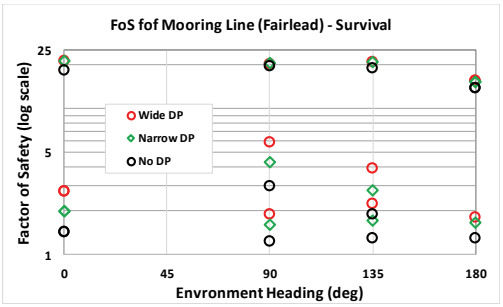

Fig. 19 Mooring Line Factor of Safeties: 500-yr Survival

CONCLUSIONS

A semi-type Y-Wind floating wind turbine platform is properly configured in order to be fabricated in US shipyards, integrated and wet-towed out to site with conventional tugs, which can give a significant cost benefit to low the platform cost. The platform can support a 5MW horizontal axis wind turbine on the center column and other three columns are connected to the center column with respective rectangular pontoon. The platform has damping plates attached to the pontoon keel which was sized accordingly to improve the platform responses but with minimizing the structural design issues. The platform was designed to be moored with three chain lines at a water depth of 200 m.

The Y-Wind design was validated with fully non-liner time domain simulations under the various DLCs in operating (rated and cutout wind), 50-yr extreme and 500-yr survival seas states in accordance with ABS wind turbine design guides. The Metocean data for those DLCs were derived from typical US offshore data available.

The numerical simulations were carried out for the Y-Wind with no damping, narrow and wide damping plate options. It is demonstrated

that the damping plate, especially wide one contributes to significantly reduce the responses in heave and roll (pitch) motions and accelerations, which also results in considerable reduction in the mooring extreme tensions. These results are very promising in the design of structural members, wind turbine components and mooring system

The Y-Wind platform with the wide damping plate is confirmed to comply with all the design criteria in motions, accelerations and mooring strengths. The present design and numerical model will be further validated with considering the fully coupled effects with the rotors and the model testing.

REFERENCES

ABS (2013). Design Guideline for Stationkeeping Systems of Floating Offshore Wind Turbines.

ABS (2015). Guide for Building and Classing – Floating Offshore Wind Turbine Installations.

ABS (2014). Guidance Notes on Global Performance Analysis for Floating Offshore Wind Turbine Installations.

ABS FPI (2013). Guide for Building and Classing Floating Production Installations.

Antonutti, R, Peyrard, C, Johanning, L, Incecik, A, and Ingram, D (2014). "An investigation of the effects of wind-induced inclination on floating wind turbine dynamics: heave plate excursion", *Ocean Engineering*, 91.

API (2007). API Bulletin 2INT-MET Interim Guidance on Hurricane Conditions in the Gulf of Mexico.

API (2005). API RP 2SK Recommended Practice for Design and Analysis of Stationkeeping Systems for Floating Structures, 2nd edition.

Boo, SY, Shelley, AS, and Kim, D (2017). "Dynamic Performance Analysis of a New Semi Type Floating Offshore Wind Turbine", *Proceedings of the 22nd Offshore Symposium*, SNAME.

Butterworth, J, Lee, JH, and Davdison, B (2004). "Experimental Determination of Modal Damping from Full Scale Testing", *13th World Conference on Earthquake Engineering*.

Cermelli, C, Aubault, A, and McCoy, T (2010). "Qualification of a Semi-Submersible Floating Foundation for Multi-Megawatt Wind Turbines", *Offshore Technology Conference*.

Cheema, A, Zhu, M, Chai, S, Chin, CKH, and Jin, Y (2014). "Motion Response of a Floating Offshore Wind Turbine Foundation," *19th Australasian Fluid Mechanics Conferenc*e.

DNV (2007) DNV RP C205 Environmental Conditions and Environmental Loads.

Fisher, FJ, and Gopalkrishman, R (1998). "Some Observations on the Heave Behavior of Spar Platforms," *17th Intl Conference on OMAE*, 1998

Fukushima FORWARD (2014). Fukushima Floating Offshore Wind Farm Demonstration Project. Japan: Fukushima Offshore Wind Consortium.

Huijs, F, Bruijin, DR, and Savenije, F (2014). "Concept Design Verification of a Semi-submersible Floating Wind Turbine Using Coupled Simulations," *Energy Procedia*, 53.

Hurley, WL and Nordstrom, C (2015). "PelaStar Cost of Energy: A cost study of the PelaStar floating foundation system in UK waters," ETI Floating Platform FEED Study Report.

Ishihara, T, and Waris, BM (2012). "Dynamic response analysis of floating offshore wind turbine with different types of heave plates and mooring systems by using a fully nonlinear mode", *Coupled Systems Mechanics*, 1, 3.

Jonkman, J (2010). "Definition of the Floating System for Phase IV of OC3," NREL Report.

Jonkman, J, Butterfield, S, Musial, W, and Scott, G (2009). "Definition of a 5-MW Reference Wind Turbine for Offshore System Development," Technical Report, NREL/TP-500-38060.

Karimirada, M and Michailides, C (2015). "V-shaped semisubmersible offshore wind turbine: An alternative concept for offshore wind technology," *Renewable Energy,* 83.

Kim, JH, Hong, SY, and Kim, HJ (2014). "The Shape Design and Analysis of Floating Offshore Wind Turbine Structures with Damper Structure and Shallow Draft," *Journal of Ocean and Wind Energy, ISOPE*.

Li, B, Huang, Z, Low, YM, and Ou, J (2013). "Experimental and numerical study of the effects of heave plate on the motion of a new deep draft multi-spar platform," *Journal of Marine Science and Technology*.

Lopez-Pavona, C and Souto-Iglesias, A (2015). "Hydrodynamic Coefficients and Pressure loads on Heave Plates for Semi-Submersible Floating Offshore Wind Turbines: a Comparative Analysis Using Large Scale Models," *Renewable Energy.*

Robertson, A, Jonkman, J, Masciola, M, Song, H, Goupee, A, Coulling, A, and Luan, C (2014). "Definition of the Semisubmersible Floating System for Phase II of OC4," NREL Technical Report, NREL/TP-5000-60601.

Roddier, D, Cermelli, C, Aubault, A, and Weinstein, A (2010). "WindFloat: a floating foundation for offshore wind turbines," *Journal of Renewable and Sustainable Energy,* 2 (3).

Statoil, https://www.statoil.com/en/what-we-do/new-energy-solutions/our-offshore-wind-projects.html

Suzuki, K, Yamaguchi, H, Akase, M, Imakita, A, and Ishihara, K (2011). "Initial Design of TLP for Offshore Wind Farm," *Journal of Fluid Science and Technology,* 6, 3.

Venugopai, V, Varyani, KS, and Westlake, PC (2009). "Drag and Inertia Coefficients for Horizontally Submerged Rectangular Cylinders in Waves and Currents," *Proc. Institution of Mechanical Engineers, Part M: J. Engineering for the Maritime Environment*, 223.

Viselli, AM, Forristall, GZ, Pearce, BR, and Dagher, HJ (2015a). "Estimation of extreme wave and wind design parameters for offshore wind turbines in the Gulf of Maine using a POT method," *Ocean Engineering*, 104.

Viselli, AM, Goupee, AJ, and Dagher, HJ (2015b). "Model Test of 1:8-Scale Floating Wind Turbine Offshore in the Gulf of Maine," *J. Offshore Mechanics and Artic Engineering*, 137.

Weinstein, A (2014). "2014 Wind Power Peer Review – Windfloat Pacific OSW Demo Project," US DoE.

Xu, K (2015). "Design and Analysis of Mooring System for Semi-submersible Floating Wind Turbines in Shallow Water," MSC Thesis, Norwegian University of Science and Technology.